energies

MDPI

Article

Boric Acid: A High Potential Candidate for Thermochemical Energy Storage

Clemens Huber [1,*], Saman Setoodeh Jahromy [1], Christian Jordan [1], Manfred Schreiner [2], Michael Harasek [1], Andreas Werner [3] and Franz Winter [1]

1 Institute of Chemical, Environmental and Bioscience Engineering, TU Wien, Getreidemarkt 9/166, 1060 Vienna, Austria; saman.setoodeh.jahromy@tuwien.ac.at (S.S.J.); christian.jordan@tuwien.ac.at (C.J.); michael.harasek@tuwien.ac.at (M.H.); franz.winter@tuwien.ac.at (F.W.)

2 Institute for Natural Sciences and Technology in the Arts, Academy of Fine Arts Vienna, Augasse 2–6, 1090 Vienna, Austria; m.schreiner@akbild.ac.at

3 Institute for Energy Systems and Thermodynamics, TU Wien, Getreidemarkt 9/302, 1060 Vienna, Austria; andreas.werner@tuwien.ac.at

* Correspondence: clemens.huber@tuwien.ac.at

Received: 15 February 2019; Accepted: 18 March 2019; Published: 21 March 2019

Abstract: This paper aims to describe the capability of the system boric acid–boron oxide for thermochemical energy storage. As part of the systematic research and in-depth analysis of potential solid/gas reaction systems, performed during the last years, this reaction system appears to be highly promising for the future of worldwide sustainable energy supply. The analysis of the reaction heat, by means of thermogravimetric and macroscopic investigations, not only showed a significantly higher energy density of 2.2 GJ/m^3, compared to sensible- and latent energy storages, but the reaction kinetic further demonstrated the reactions' suitability to store energy from renewable energy and waste heat sources. This paper, therefore, shows a new approach regarding the application of the boric acid–boron oxide reaction system and elaborates on the advantages and challenges for its use as energy storage.

Keywords: thermochemical energy storage; boric acid; boron oxide; thermogravimetric analysis; ICTAC

1. Introduction

It lies within human nature to stick to accustomed patterns as long as they bring the desired result, despite knowing about the potential severe consequences for the future. Acting usually starts only when time is already close of running out. The steady rise of the global energy demand and the rise of the global air pollution are closely interlinked and one of the greatest challenges of the present. Emitting gases like carbon dioxide or nitrogen oxides are, therefore, rightly doomed for their contribution to environmental pollution and an increase of the global warming effect with severe consequences, such as rising sea levels, droughts, floods, or hurricanes.

It took politics until the end of the 20th century to slowly recognise global warming and its harmful impact as a serious global threat. The Kyoto Protocol concluded in 1997 was one of the first international political confessions concerning environmental protection, with a legal obligation to reduce greenhouse gas (GHG) emissions [1]. It was followed by further regulations, national commitments, and activities, such as the Europe 2020 strategy or the 2030 climate energy framework [2,3]. Renewable energy sources and the promotion of efficiency measures are thereby seen as key tasks for a sustainable reduction of GHG emissions.

It is expected, that the global demand for energy will rise by 30% until the year 2040. Additionally, there will be a slight increase of energy related CO_2 emissions [4]. To meet the defined targets, many

different strategies and schemes are necessary. Due to the fact, that a very large proportion of CO_2 emissions originates from industrial processes the usage of industrial waste heat—a hitherto largely unused energy source—would be one possible step into the right direction. Waste heat definitely has the potential to at least satisfy the energy demand of private homes. Miro et al. [5] already described the large potential of industrial waste heat as significant and despite some slight data inaccuracies, he leaves no doubt about its significance for future energy supply.

While already various powerful CO_2 free energy sources can be found around the world, such as solar energy, wind, geothermal energy, and hydro- or tidal power, they are all limited by one major drawback: the energy release depends on geographic locations, seasons, or daytimes and does not take into account the actual energy demand. If it cannot be used in the moment of its release, or stored for further usage, this energy gets simply lost to the environment and converts to anergy (useless energy at the ambient level).

Keeping this in mind, there is the urgent necessity to bridge the time gap between the provision of thermal energy (renewable and waste heat) and the varying energy demand. Thermal energy storages systems (TES) will, therefore, play a significant role in the future. At present, there are several methods for storing thermal energy such as sensible, latent or thermochemical heat storage systems (see inter alia [6–9]). Sensible heat storages use the high specific heat capacity for storing thermal energy, while the mechanism of latent heat storages is based on a phase change process (mainly solid–liquid or liquid–gas).

Thermochemical energy storage systems are still at an experimental stage, whereas the other TES' are relatively well studied and mostly market ready. Nevertheless, they all share the common disadvantage of a huge energy loss. Due to the laws of thermodynamic (e.g., Fourier's law) storing energy at a higher temperature level, compared to the environment, leads to an unstoppable energy loss. Hence, storage time is limited and there is a strong need for proper insulation.

Due to their much higher energy density compared to ordinary storage systems, thermochemical energy storage (TCES) recently experienced particular scientific attention. Within the TCES, one can distinguish between two different types of storage systems, based on their mechanism; physical sorption processes and chemical reaction processes. For the scope of this paper, TCES only comprises chemical reaction processes.

TCES processes use the energy of reversible chemical reactions and the stored amount of energy is equal to the reaction enthalpy. During the endothermic charging process, thermal energy gets absorbed and decomposes a chemical compound A, into two products -B and C:

$$\nu_A A + \Delta H_R \rightleftarrows \nu_B B + \nu_C C \quad (1)$$

The products obtained through this reaction, contain the reaction enthalpy and are ready to be stored at ambient temperature. By turning back into A in the course of an exothermic reaction, B and C release the previously stored energy whenever needed and can then be charged again (Figure 1). To facilitate the separation of the products, one of the products B or C is preferably a solid and the other one a gas. In case, the gas is easily available, the storage volume could be significantly reduced by storing only the solid product.

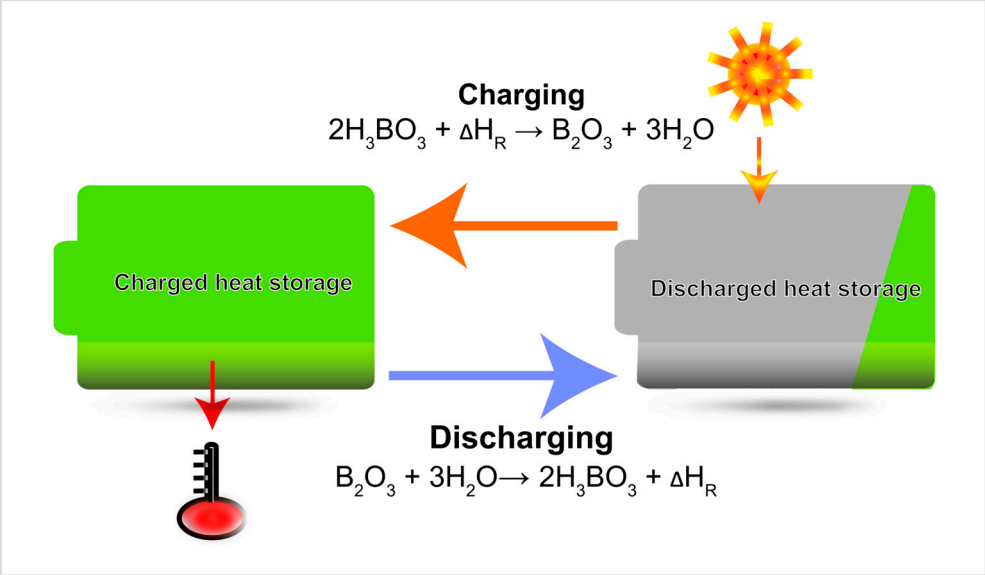

Figure 1. Schematic thermochemical energy storage process illustrated by the boric acid/boron oxide reaction.

Characteristics like reversibility, the rate of reaction, operation conditions, and the reaction kinetics are necessary information to determine whether a substance is suitable to serve as TCES [9]. A small molar volume paired with a large reaction enthalpy, further maximizes the thermal storage capacity. Additionally, no side reactions should affect the reaction turnover and a good cycle stability should preserve the energy storage density over a long period of time [6].

Nevertheless, there is still no technology yet market ready to bridge the time gap, between the potential energy deriving from industrial waste heat or sustainable energy sources, and the selective energy demand. To reach this goal, new ways for a sustainable energy supply need to be found, and in particular TCES storage technologies should become the focus of attention. Studies regarding the boric acid–boron oxide reaction system were primarily driven so far by the industrial sector (e.g., glass. ceramics, fire protection). This paper wants to present a new promising approach of boric acid and its suitability as TCES system. Research results regarding the characteristics of the material will provide the basis for further investigations.

2. Materials and Methods

2.1. Discovery and Mechanism

The work of Deutsch et al. [10], who developed a new systematic search algorithm for thermochemical storage materials, provided the basis for the discovery of this reaction. They applied a mathematical search algorithm to a chemical database for identifying potential solid/gas reactions. Due to practical reasons, they further narrowed the scope to reactions of solid inorganic substances with a defined gaseous reactant, and thereby revealed more than a thousand unique reactions. Limiting the equilibrium temperature of this reactions to 1000 °C, and taking further limitations like heat storage capacity, availability, and the price into account, yielded a final list of potential reaction systems. To proof their real suitability as TCES, the listed reaction systems were briefly analysed—using different analytical techniques—and then ranked in respect to their characteristics.

As a result, the reaction system B_2O_3/H_3BO_3 was further investigated. Due to its high energy density of 2238 MJ/m^3 and the apparent possibility to assure a complete conversion over an endless number of reaction cycles, strongly differed it from other reaction systems. Table 1 summarizes different thermal energy storage systems (TES).

Table 1. Comparison of different thermal energy storage systems (TES).

Type	Material	Energy Storage Density	Temp-Range/Melting Point	Ref.
Physisorption TES	Zeolites 13X/H_2O	601 MJ/m^3	65–130 °C	[11]
Chemisorption TES	$MgSO_4 \times 7H_2O$	1512 MJ/m^3	150 °C	[11]
Sensible TES	HITEC solar salt	2.9 MJ/m^3	250–450 °C	[12]
Sensible TES	Water at 50 °C	206 MJ/m^3	50 °C	[13]
Latent TES	$MgCl_2$	1048 MJ/m^3	714 °C	[14]
Latent TES	NaF	2031 MJ/m^3	996 °C	[6]
TCES	Cu_2O	3606 MJ/m^3	350–1100 °C	[15]
TCES	H_3BO_3	2238 MJ/m^3	90–<200 °C	[16]

The reaction mechanism of boric acid (H_3BO_3)–boron oxide (B_2O_3)—with the intermediate metaboric acid (HBO_2)—is still not fully and clearly examined. On one hand, Zachariasen [17] described three crystalline modifications of metaboric acid. According to this theory, that was also represented inter alia by Sevim et al. [18], Balcı et al. [19] or Zhang et al. [20], the thermal decomposition of boric acid by thermogravimetric analysis (TG) would reveal two distinguished steps:

$$2H_3BO_3 \rightarrow 2HBO_2 + 2H_2O \uparrow \quad (2)$$

$$2HBO_2 \rightarrow B_2O_3 + H_2O \uparrow \quad (3)$$

On the other hand, while studying different crystalline structures of boric acid, Harabor et al. [21] observed three different thermal induced reactions. The mass loss was attributed to each of this reaction steps. Within this new approach different crystalline modifications of boric acid were analysed, however, in this case the crystalline modifications of metaboric acid appear to be insignificant for the reaction [22,23]:

$$H_3BO_3 \rightarrow HBO_2 + H_2O \uparrow \quad (4)$$

$$HBO_2 \rightarrow \frac{1}{4}H_2B_4O_7 + \frac{1}{4}H_2O \uparrow \quad (5)$$

$$\frac{1}{4}H_2B_4O_7 \rightarrow \frac{1}{2}B_2O_3 + \frac{1}{4}H_2O \uparrow \quad (6)$$

2.2. Occurrence and Application of B_2O_3/H_3BO_3

Borate minerals occur in regions with volcanic activity and arid climate. The minerals mainly used by the industry are:

- Colemanite $Ca[B_3O_4(OH)_3] \times H_2O$
- Kernite $Na_2[B_4O_6(OH)_2] \times 3H_2O$
- Tincal $Na_2[B_4O_5(OH)_4] \times 8H_2O$
- Ulexite $CaNa[B_5O_6(OH)_6] \times 5H_2O$

In 2017, the annual global production volume of boron was about ten million metric tons (excluding the amount of the US production), mainly supplied from countries such as Turkey, Peru, Chile or Argentina. Global (explored) reserves of at least one billion tons can be found in North- and South America, as well as in regions in South- and Central Asia [24]. A future increase in demand for boron compounds would lead to further explorations of potential deposits all over the world (e.g., Serbia, Iran) [25]. Nearly 75% of the worldwide borate consumption concerns the production of ceramics, detergents, fertilizers, and (heat-resistant) glass [24]. In addition to this area of application, it is further used for mineral wool, sport equipment, insecticides, or medical treatments [26–28]. Furthermore, there were investigations regarding its usage as rocket propulsion or military use [29].

As already mentioned above, the material properties of a chemical compound are strongly affecting the performance of the thermal energy storage. Therefore, various influencing parameters for an energy storage process have to be taken into account, such as: melting point, density, latent heat of

fusion, specific heat, thermal conductivity, cost, availability, thermal and chemical stability, volume change, toxicity, corrosiveness, as well as many others [7].

2.3. Material Properties

2.3.1. Material

The analysed sample material was taken from:

- Boric Acid: Sigma Aldrich (St. Louis, MO, USA) (11606/CAS: 10043-35-3)
- Boron Oxide: Alfa Aesar (Wardhill, MA, USA) (12290/CAS: 1303-86-2)
- Metaboric Acid: Santa Cruz Biotechnology (Dallas, TX, USA) (sc-228460/CAS: 13460-50-9)

The purity of the samples—declared by the manufacturer—was above 99%. This was checked inter alia by means of inductive plasma mass spectroscopy (ICP), trace metal analyses and acidimetric titration. Since the standardized detection methods by titration does not distinguish between boron oxide, metaboric acid or boric acid, a possible degradation of boron oxide due to its hygroscopic behaviour—e.g., with humidity—could neither be detected nor excluded.

2.3.2. Particle Size

The particle size of boric acid and boron oxide was analysed by a laser diffraction measurement device (Mastersizer 2000, Malvern Instruments, Malvern, UK). Equipped with a dry dispersion module Scirocco 2000), using air for particle-in-gas sizing, it provided an analysis of the particle size in the interval between 0.020 and 2000 µm. Boron oxide was analysed twice, before and after one hour of milling with a ball mill.

2.3.3. Scanning Electron Microscopy

For a deeper insight into the sample structure, a scanning electron microscope device (SEM) (FEI Quanta 250 FEGSEM) was used for imaging the particle surface. To ensure pure samples, boron oxide was initially thermally pre-treated (300 °C for 10 h).

2.3.4. X-Ray Diffraction Analysis

To analyse the sample material, powder X-ray diffraction measurements (XRD) were carried out on a PANalytical X'Pert Pro diffractometer in Bragg-Brentano geometry using a mirror for separating the Cu Kα1,2 radiation and an X'Celerator linear detector. For in situ monitoring of experiments an Anton Paar HTH1200N chamber was used.

2.3.5. Thermal Conductivity/Diffusivity

Daniel Lager [30] further investigated the thermal conductivity of this reaction system. He examined the thermal conductivity of boron oxide and boric acid by using a laser flash analysis (LFA) device (NETZSCH LFA 467), as well as a Transient Hot Bridge (THB) analysing device (Linseis THB 100). Bulk samples of H_3BO_3 and B_2O_3 (ρ = 951 and 1280 kg/m^3) have been analysed via the THB device, whereas LFA technique has been applied to pressed pellet samples of H_3BO_3 (ρ = 1436 kg/m^3).

2.3.6. Reaction Heat Analysis

All the experimental examinations of the thermochemical reaction were performed by a simultaneous thermal analysis (STA) device (Netzsch STA449 Jupiter), equipped with a TGA-DSC sample holder. The oven allowed experimental investigations with temperatures ranging from 25 °C to 1250 °C, regulated by an S-Type thermocouple. Mass flow meters (Red-y smart, Voegtlin, Aesch, Switzerland) were used to control the gas flow rate of nitrogen. Aluminium oxide crucibles without lids (Ø = 6 mm, 75 µL) were used for all experiments. Furthermore, nitrogen as inert gas with a

flow rate of 100 mL/min was adjusted for each experimental run. Equipped with a steam generator, the instrument allowed thermal investigations under defined moist conditions.

The analysis of the hydration reaction was performed under isothermal conditions while adding a predefined water vapour mass flow to the gas flow. The dehydration process was examined under non isothermal conditions (2, 4 and 8 K/min). According to the recommendations of the International Confederation for Thermal Analysis and Calorimetry (ICTAC) Kinetics Committee, the mass should be kept as small as possible to ideally obtain results not influenced by the sample mass [31]. Therefore, a sample mass of 2 mg was used for all experiments. In addition, preliminary studies with various sample masses were performed, to estimate the significance of the mass influence on the result.

2.3.7. Macroscopic Reaction Heat Analysis

A simple experimental setup (Dewar reactor) was realized for the analysis of the hydration reaction comprising: a Dewar vessel with a capacity of one litre (Agil 1, Air Liquide, Paris, France) a stirrer and a thermocouple with a logging function (Figure 2). The process was started, by feeding water from the vessel lid triggering the exothermal reaction.

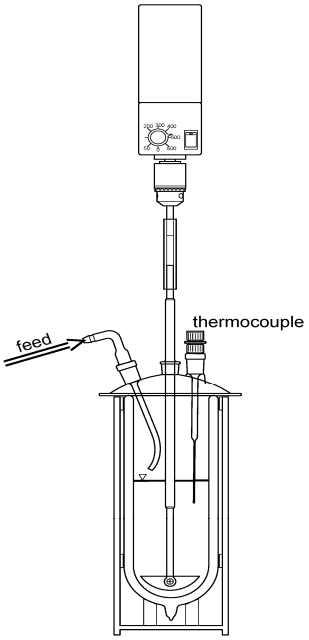

Figure 2. Dewar reactor—Set up for macroscopic reaction heat analysis.

3. Results

3.1. Particle Size

Figure 3 shows the measured particle size distribution (Frequency) and the cumulative frequency (Sum) of the analysed samples. Due to the great hardness of B_2O_3—in the range of 1.5 GPa for amorphous and ten times higher for the high pressure configuration [32]—no significant effect of milling—whether on particle size nor on distribution—was noticed. The metaboric acid sample apparently consisted of amorphous fragments. Therefore, it was excluded from particle size analyses.

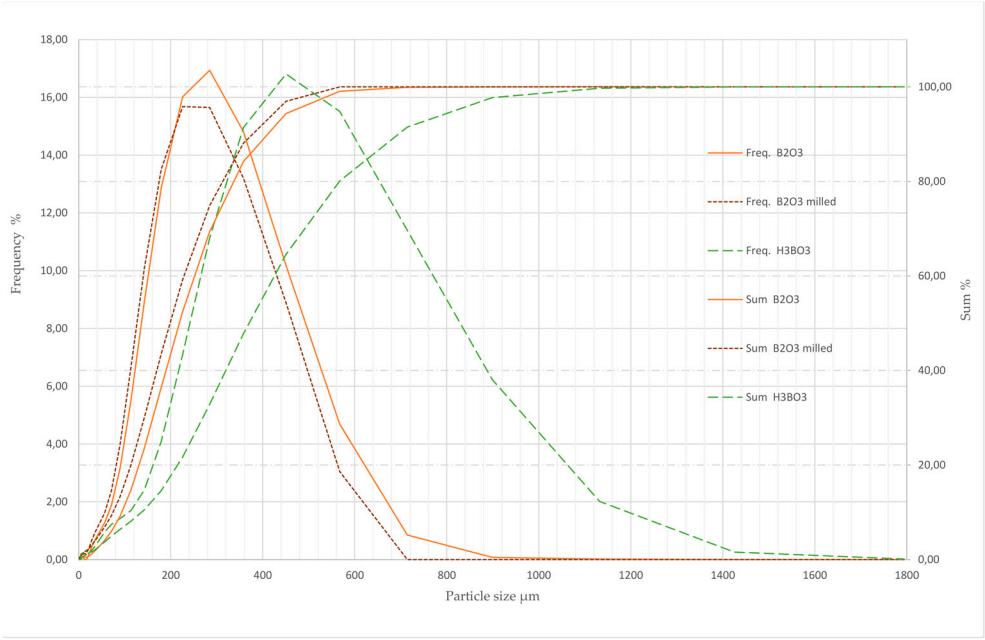

Figure 3. Particle size distribution of B_2O_3 (before and after milling) and H_3BO_3 samples.

3.2. Scanning Electron Microscopy (SEM)

The images of boric acid revealed a rather round shape and a clean and smooth, plate-shaped surface (Figure 4). Boron oxide and metaboric acid showed an angular particle shape and an apparent porous surface. The angular particle shape is very likely a result of grinding and therefore the samples have been assumed vitreous. The images have been taken with an accelerating voltage of 2.5 kV at a working distance between 10.2 and 10.4 mm.

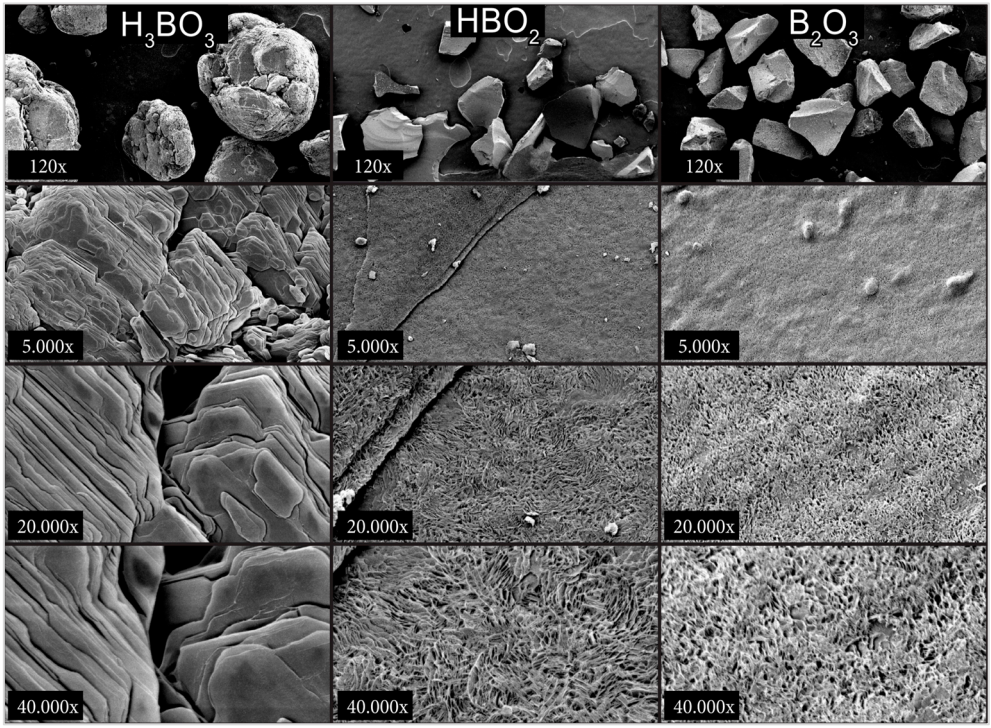

Figure 4. SEM images of H_3BO_3 (first column), HBO_2 (second column) and B_2O_3 (third column) at different resolutions (lines) of 120×, 5000×, 20,000×, and 40,000× (accelerating voltage: 2.5 kV).

3.3. X-Ray Diffraction Analysis

The XRD analysis showed the purity of the used boric acid and identified the samples monoclinic crystal system (Figure 5). However, an analysis of boron oxide was not possible due to its obvious amorphous structure. This would correspond with the SEM results as boron oxide is produced by dehydration of boric acid. In this process, the boric acid gets heated up to 1000 °C and causes a melting of the solid. The resulting vitreous boron oxide gets, after cooled down, ground, and sieved. The amorphous structure with randomly distributed atoms scatter X-rays in many directions and therefore causes only a large bump (Figure 6).

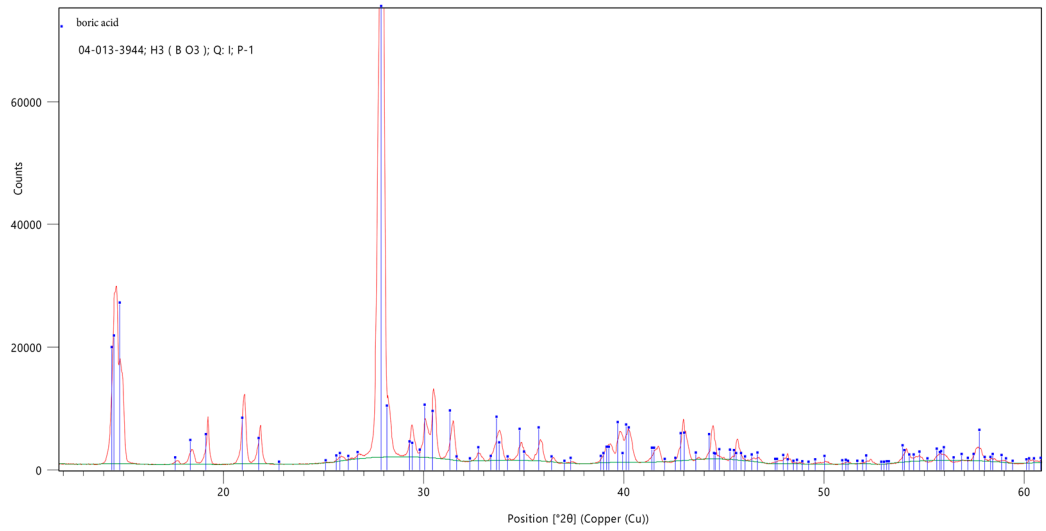

Figure 5. X-ray diffraction analysis of monoclinic boric acid.

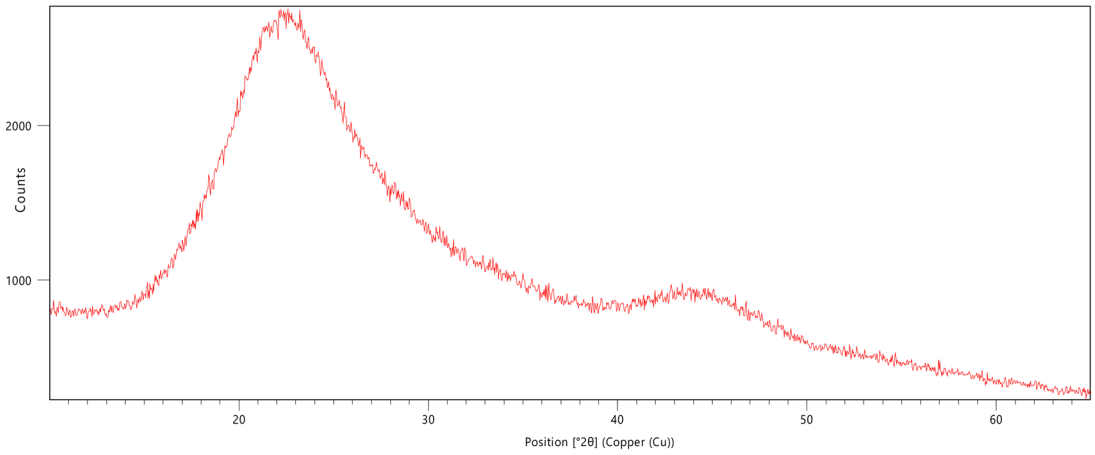

Figure 6. X-ray diffraction analysis of amorphous boron oxide.

3.4. Thermal Conductivity/Diffusivity

Figure 7 shows the thermal diffusivity of boric acid. The thermal diffusivity decreases with rising temperatures until fifty degrees, as well as the thermal conductivity calculated from this data. The THB analysis shows a temperature influenced increase in thermal conductivity for boron oxide and boric acid. The increase in the standard deviation of boric acid, at temperatures above 70 degrees, could be a result of boric acid decomposing to metaboric acid and vapour. Since the convective share of the heat transport is related to the gas flow velocity, the evolving water vapour causes a stochastic turbulent gas flow in the bulk sample, hence, influencing the apparent thermal conductivity of the bulk material.

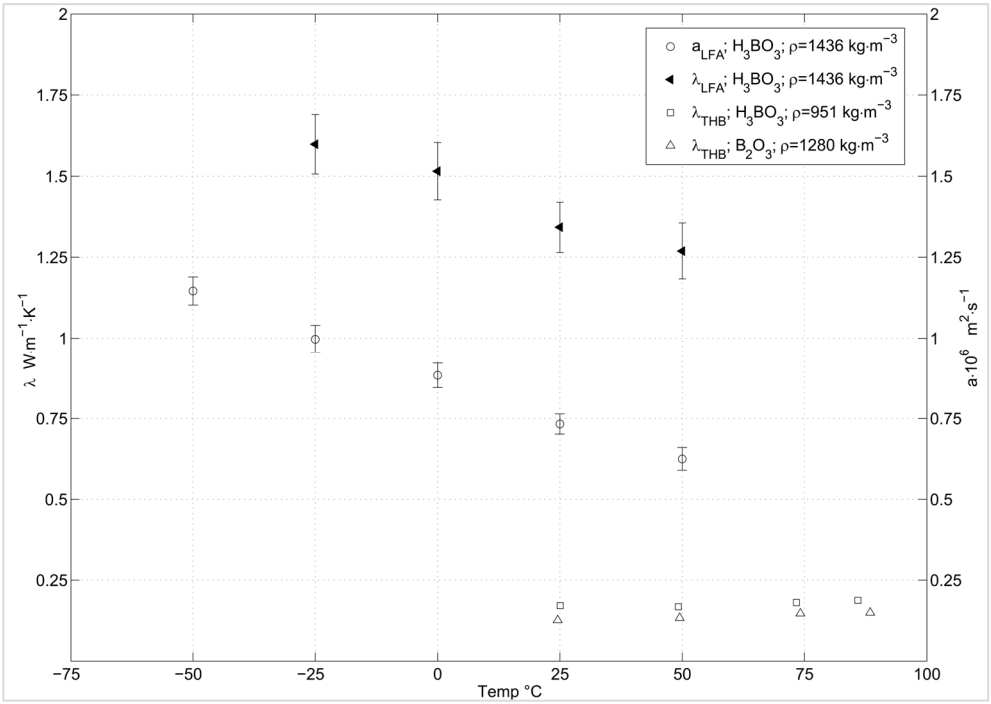

Figure 7. Thermal conductivity (λ) and thermal diffusivity (a × 10^6) for B_2O_3 and H_3BO_3 (pellet and powder) [30].

3.5. Reaction Heat Analyses

3.5.1. Hydration

Experiments to investigate the hydration reaction of boron oxide, revealed an apparent evaporation of the resulting boric acid in the presence of water vapour. Thus, an accurate analysis of the hydration process of boron oxide became impossible. Walter Dressler [33] analysed the volatility of boric acid in relation to water content and temperature. He was one of the first who described the influence of temperature and varied boric acid concentrations in water on the volatility inter alia by steam distillation. Even low concentrations lead to an evaporation of boric acid and further increasing linear with a rising concentration.

To verify this theory, isothermal experiments with various temperatures and steam content were performed. Hydration experiments of boron oxide showed a mass loss, influenced by temperature, initial mass and steam content. The first mass increase, due to formed boric acid, is then followed by a mass loss due to its vaporization. This mass loss is apparently influenced by temperature (Figure 8) and water vapour content (Figure 9). The higher the temperature and/or steam content (including the evolving water vapour from the boric acid decomposition), the faster the mass reduction of the reacted boric acid.

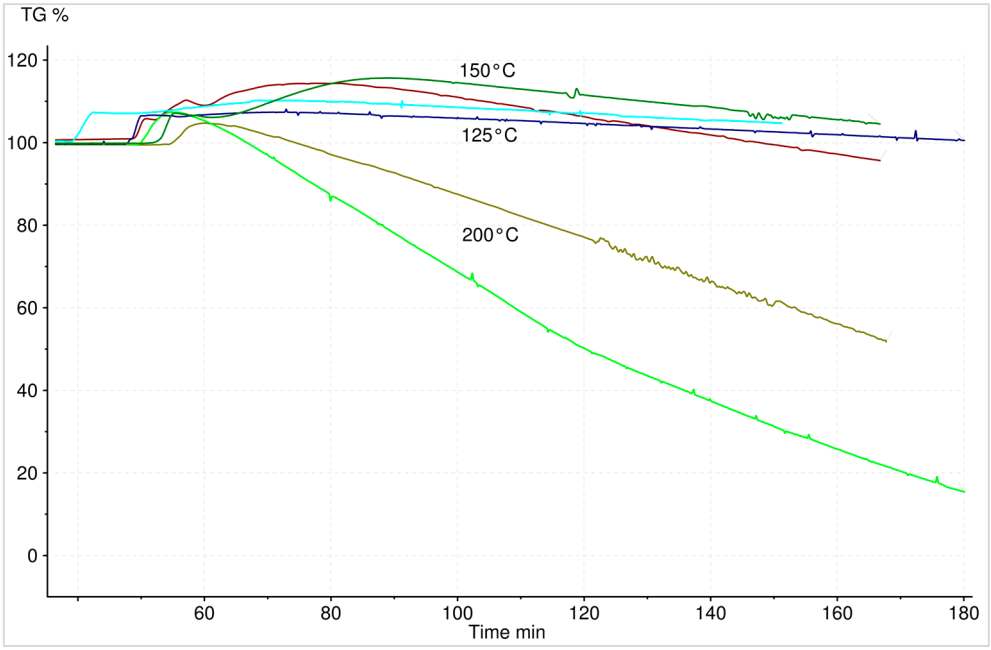

Figure 8. Hydration of 9.8 and 1.3 mg B_2O_3 at constant water vapour mass flow (5 g/h H_2O within 100 mL/min N_2)—temperature influence on the volatility of the resulting H_3BO_3.

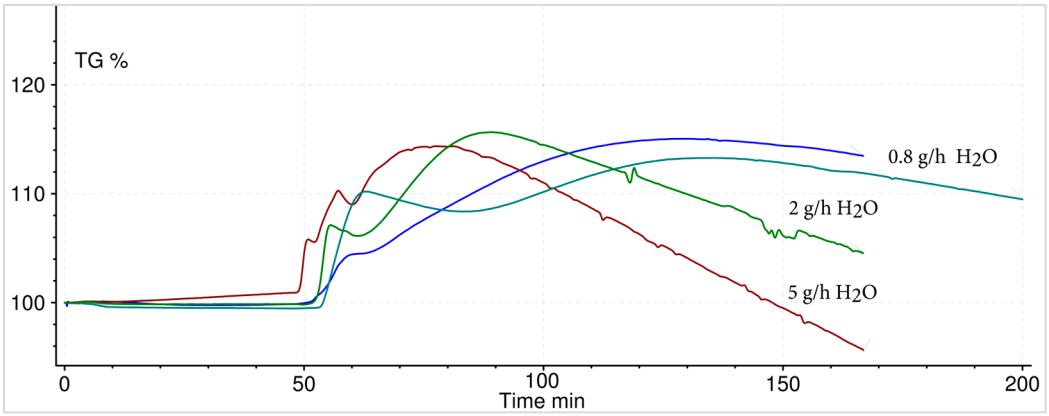

Figure 9. Hydration of 10 mg B_2O_3 at constant temperature of 150 °C—volatility of the resulting H_3BO_3 depending on various water vapour mass flows.

Experiments to quantify the volatility of boric acid without added water vapour have been conducted. Therefore, boric acid was thermal decomposed (up to 200 °C) in a flask, under a defined nitrogen gas flow (100 L/h) and defined pressure conditions. Analysing the deposited mass of boric acid, by weighting each individual component of the experimental set up, before and after the experiment, revealed that even the evolving vapour of the decomposition is sufficient to cause a relative mass loss of around one percent during a period of 40 minutes (Figure 10).

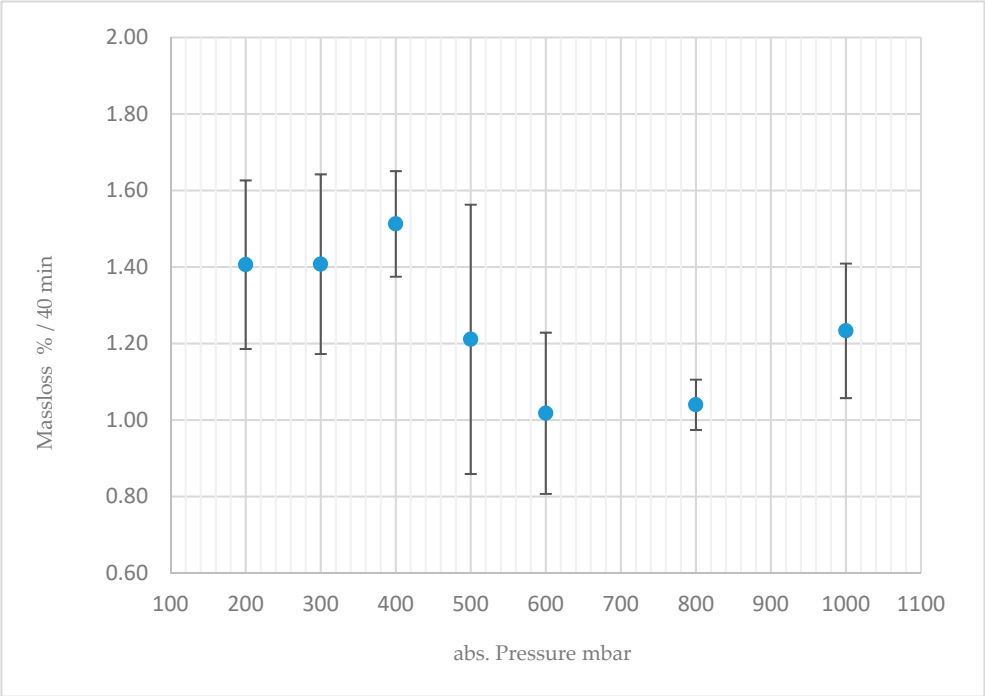

Figure 10. Volatility of 2.5 mg boric acid heated up to a temperature of 200 °C, as a function of absolute pressure [34].

3.5.2. Dehydration

Comparing different experimental results with varying initial sample masses (2 mg, 13.1 mg, and 16.6 mg) revealed a significant influence of the sample mass on the measurement results (Figure 11). For that reason, it was conclusive to conduct the experiments with a sample mass of 2 mg. On average the results for the decomposition reaction showed a specific energy content of 1.7 GJ/m^3 (Figure 12). The cause for the significant difference between the theoretical (2.2 GJm^3) and experimental (~1.7 GJ/m^3) specific energy content of boric acid, might be the usage of an open crucible for the thermal analysis (energy losses to gas stream). Contrary to the hitherto published results, the use of lower sample masses yielded a shift of the reaction to lower temperatures. The results revealed a reaction temperature range (depending on the heat rate), from 70 °C to 200 °C. Additionally, no difference to the classical approach of the intermediate reaction (two or three steps with mass loss) could be noticed (Figure 13).

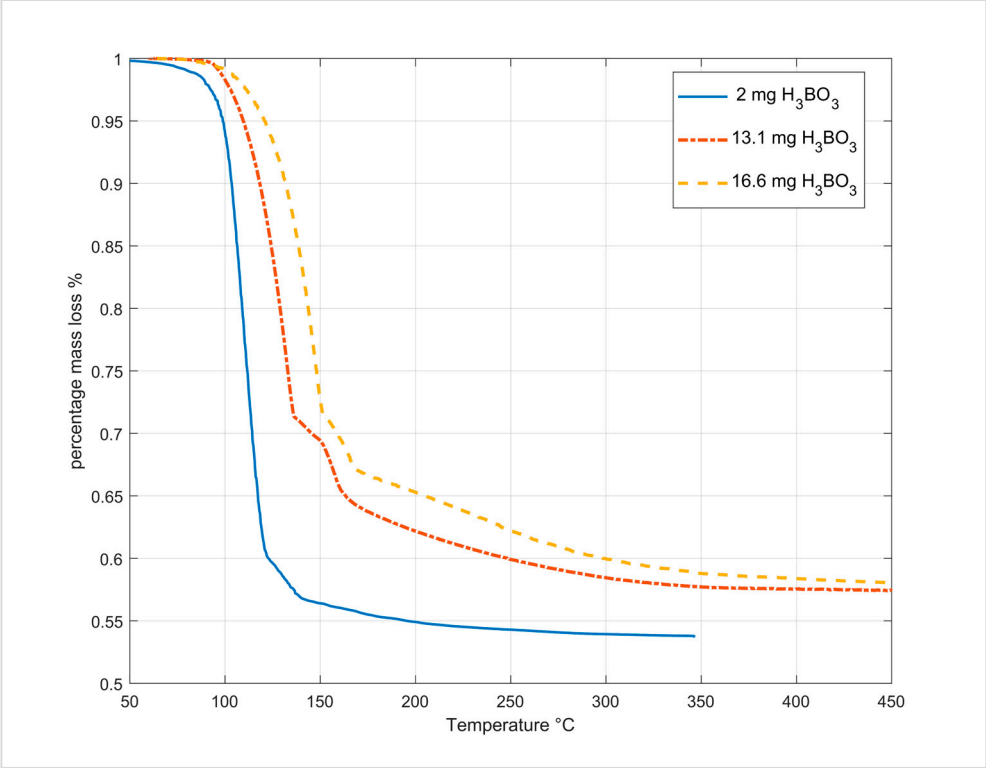

Figure 11. Dehydration (TG) of boric acid at a heating rate of 2 °C/min subject to different initial masses.

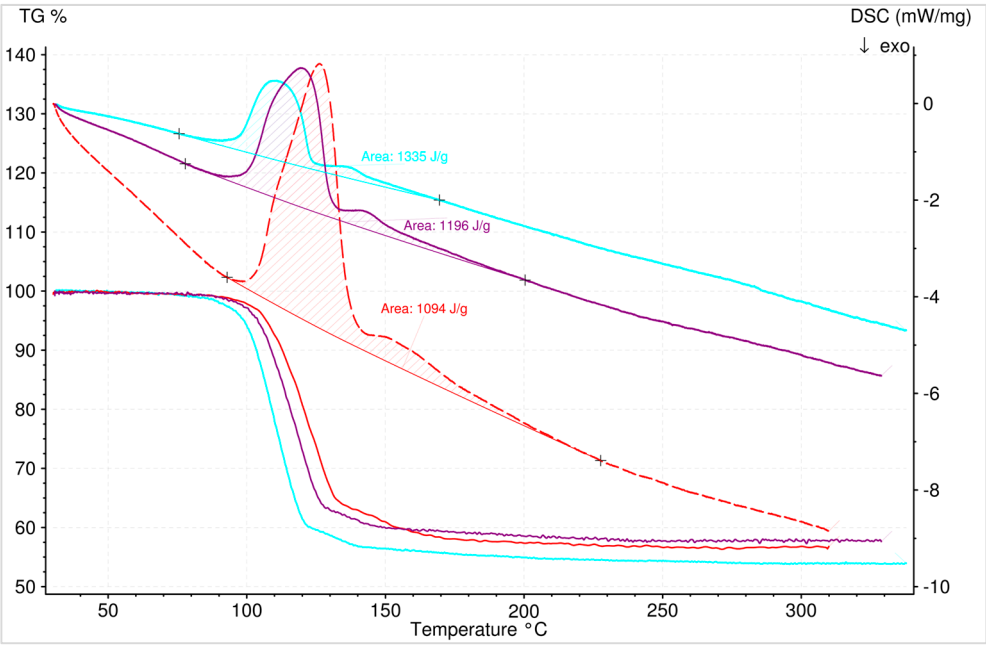

Figure 12. Dehydration (TG and DSC) of 2 mg H_3BO_3 at different heating rates of 2 (turquoise), 4 (violet), and 8 °C/min (red) with the specific energy content of the reaction (1.3, 1.2, and 1.1 KJ/g).

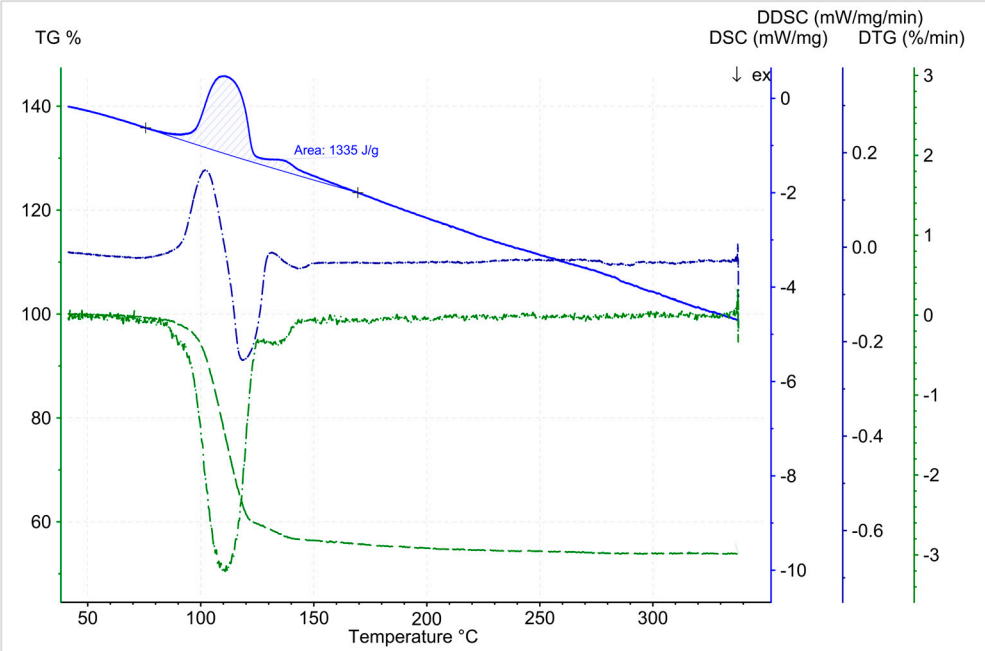

Figure 13. Temperature-dependent dehydration start of 2 mg H_3BO_3 at a heating rate of 2 °C/min (TG, DSC, DTG, DDSC). Specific energy content of the reaction: 1.3 KJ/g.

3.6. Macroscopic Reaction Heat Analysis

Experiments using a stoichiometric ratio of water caused a strong increase of the viscosity due to agglomeration (caking), as well as a decreasing mixing quality. This led to an overload stop of the mixer before achieving a full conversion. The agglomeration further caused a poor quality of the measured thermal signal. Hence, to achieve a homogeneous reaction progress through the reactor and a full conversion, the strong hygroscopic behaviour of boron trioxide called for a water surplus ratio in the range between five to thirty (Equation (7)).

The water surplus λ is defined by the molar amount of water (n_{H_2O}) and boron oxide ($n_{B_2O_3}$) as:

$$\lambda = \frac{n_{H_2O}}{3} * \frac{1}{n_{B_2O_3}} \quad (7)$$

In comparison to a surplus of 10, a surplus of five led to a doubled temperature increase (more than 40 °C), with a nearly full conversion (Figure 14). Figure 15 shows the influence of the initial temperature and the water surplus on the resulting temperature. Providing a full conversion, with a lower initial temperature enables a higher rise of temperature, while at initial temperatures above 70 °C there was no further measurable temperature rise.

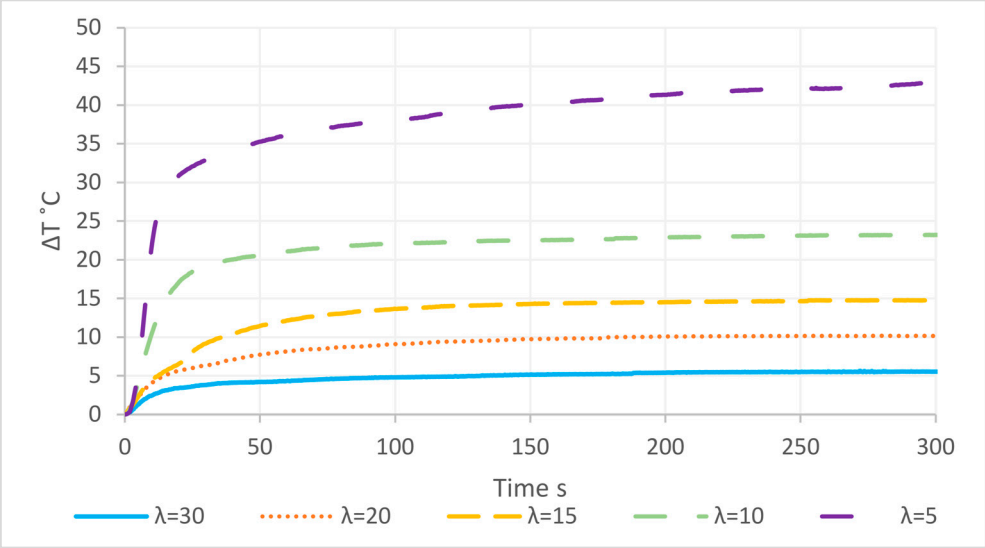

Figure 14. Temperature rise of the hydration reaction depending on different water surplus ratios (λ) with a common initial temperature of 25 °C [35].

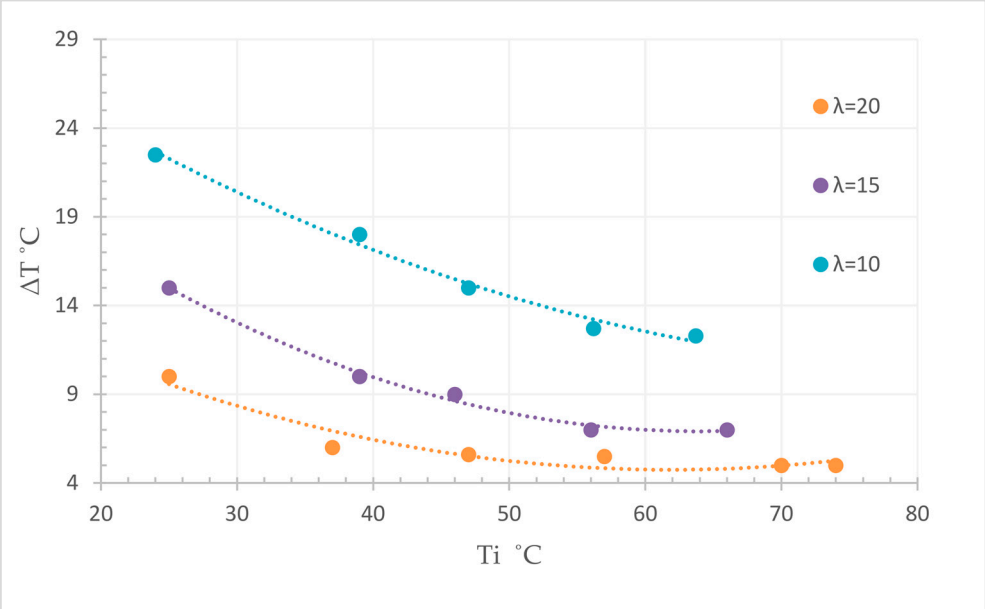

Figure 15. Total temperature rise of the hydration reaction as a function of water surplus λ (20, 15, and 10) and initial temperature T_i [35].

A further decrease of the water surplus while simultaneously solving the agglomeration problem enables a further significant increase of the resulting temperature. Due to this strong influence on the reaction, appropriate storage conditions are necessary to avoid a degradation of the reactant and to guarantee the best reaction kinetic and conservation of the stored energy.

4. Conclusions

The outcome of these investigations demonstrates the capability of the boric acid–boron oxide reaction for the application as thermochemical storage system. Compared to other thermal energy storage systems, the system shows a very high theoretical energy density of 2.2 GJ/m^3 (measured with losses: 1.7 GJ/m^3) without significant problems for a storing process. Therefore, it is a suitable candidate for thermal energy storage. Even if there is still a lot of work to do until then, it definitely has a strong potential to meaningfully contribute to a global sustainable energy supply. In addition,

the analysis with reduced sample masses has shown a significant reduction of the measured reaction temperatures. In accordance with the recommendations of the International Confederation for Thermal Analysis and Calorimetry (ICTAC), the resulting temperature for the decomposition reaction ranges between 70 °C and 200 °C. Furthermore, no evidence regarding the presence of more than two thermally-induced steps of decomposition could be found. Unfortunately, the volatility of the material in the presence of water vapour impeded a thermogravimetric analysis of the hydration process, which is why the results did not show the full (theoretical) potential of the reaction.

However, the experimental results using a Dewar reactor and a water surplus, to ensure a good mixing quality and a complete conversion, granted promising results for the future.

5. Patents

As result of this research, the application of this reaction system as thermochemical storage system was patented [36].

Author Contributions: Conceptualization: C.H.; data curation: C.H.; formal analysis: C.H. and S.S.J.; investigation: C.H., S.S.J., and C.J.; methodology: C.H. and S.S.J.; project administration: M.H. and A.W.; resources: S.S.J., M.H., A.W., and F.W.; software: C.H. and S.S.J.; supervision: M.H., A.W., M.S., and F.W.; validation: S.S.J. and C.J.; visualization: C.H.; writing—original draft: C.H.; writing—review and editing: C.H., S.S.J., C.J., M.S., and F.W.

Funding: Austrian Research Promotion Agency (FFG), SolidHeat Pressure (#853593), SolidHeat Kinetics (#848876), and SolidHeat Basic (#841150).

Acknowledgments: The authors thank the Austrian Research Promotion Agency (FFG) for the financial support of the project SolidHeat Kinetics (848876) and SolidHeat Pressure (853593. The Universitäre Service-Einrichtung für Transmissions Elelektronenmikroskopie (USTEM) and the X-Ray Center (XRC) of TU Wien are acknowledged for providing access to the scanning electron microscopy (SEM) and powder X-ray diffractometers. Many thanks to the research group of Mechanical Engineering and Clean Air Technology of the institute for providing the Mastersizer 2000 for measuring the particle size distribution of samples. The authors acknowledge the TU Wien University Library for financial support through its Open Access Funding Program.

Conflicts of Interest: The authors declare no conflict of interest.

References

1. UNFCCC. What Is the Kyoto Protocol? Available online: https://unfccc.int/process-and-meetings/the-kyoto-protocol/what-is-the-kyoto-protocol/what-is-the-kyoto-protocol (accessed on 6 August 2018).
2. European Commission. 2020 Energy Strategy. Available online: https://ec.europa.eu/energy/en/topics/energy-strategy-and-energy-union/2020-energy-strategy (accessed on 6 August 2018).
3. European Commission. 2030 Climate & Energy Framework. Available online: https://ec.europa.eu/clima/policies/strategies/2030_en#tab-0-0 (accessed on 7 August 2018).
4. International Energy Agency. *World Energy Outlook 2017*; International Energy Agency: Paris, France, 2017.
5. Miro, L.; Bruckner, S.; Cabeza, L.E. Mapping and discussing Industrial Waste Heat (IWH) potentials for different countries. *Renew. Sustain. Energy Rev.* **2015**, *51*, 847–855. [CrossRef]
6. Alva, G.; Liu, L.K.; Huang, X.; Fang, G.Y. Thermal energy storage materials and systems for solar energy applications. *Renew. Sustain. Energy Rev.* **2017**, *68*, 693–706. [CrossRef]
7. Alva, G.; Lin, Y.; Fang, G. An overview of thermal energy storage systems. *Energy* **2018**, *144*, 341–378. [CrossRef]
8. Zhang, H.L.; Baeyens, J.; Caceres, G.; Degreve, J.; Lv, Y.Q. Thermal energy storage: Recent developments and practical aspects. *Prog. Energy Combust. Sci.* **2016**, *53*, 1–40. [CrossRef]
9. Pardo, P.; Deydier, A.; Anxionnaz-Minvielle, Z.; Rouge, S.; Cabassud, M.; Cognet, P. A review on high temperature thermochemical heat energy storage. *Renew. Sustain. Energy Rev.* **2014**, *32*, 591–610. [CrossRef]
10. Deutsch, M.; Muller, D.; Aumeyr, C.; Jordan, C.; Gierl-Mayer, C.; Weinberger, P.; Winter, F.; Werner, A. Systematic search algorithm for potential thermochemical energy storage systems. *Appl. Energy* **2016**, *183*, 113–120. [CrossRef]
11. Cabeza, L.F.; Sole, A.; Barreneche, C. Review on sorption materials and technologies for heat pumps and thermal energy storage. *Renew. Energy* **2017**, *110*, 3–39. [CrossRef]

12. Gonzalez-Roubaud, E.; Perez-Osorio, D.; Prieto, C. Review of commercial thermal energy storage in concentrated solar power plants: Steam vs. molten salts. *Renew. Sustain. Energy Rev.* **2017**, *80*, 133–148. [CrossRef]
13. *VDI-wärmeatlas, V. 10. Auflage*; Springer: Berlin, Germany, 2006.
14. Zalba, B.; Marin, J.M.; Cabeza, L.F.; Mehling, H. Review on thermal energy storage with phase change: Materials, heat transfer analysis and applications. *Appl. Therm. Eng.* **2003**, *23*, 251–283. [CrossRef]
15. Setoodeh Jahromy, S.; Birkelbach, F.; Jordan, C.; Huber, C.; Harasek, M.; Werner, A.; Winter, F. Impact of Partial Pressure, Conversion, and Temperature on the Oxidation Reaction Kinetics of Cu_2O to CuO in Thermochemical Energy Storage. *Energies* **2019**, *12*, 508. [CrossRef]
16. Roine, A. *HSC Chemistry® 7*; Outotec: Espoo, Finland, 2007.
17. Zachariasen, W.H. The crystal structure of cubic metaboric acid. *Acta Crystallogr.* **1963**, *16*, 380–384. [CrossRef]
18. Sevim, F.; Demir, F.; Bilen, M.; Okur, H. Kinetic analysis of thermal decomposition of boric acid from thermogravimetric data. *Korean J. Chem. Eng.* **2006**, *23*, 736–740. [CrossRef]
19. Balcı, S.; Sezgi, N.A.; Eren, E. Boron Oxide Production Kinetics Using Boric Acid as Raw Material. *Ind. Eng. Chem. Res.* **2012**, *51*, 11091–11096. [CrossRef]
20. Zhang, W.; Sun, S.; Xu, J.; Chen, Z. Kinetic Study of Boron Oxide Prepared by Dehydration of Boric Acid. *Asian J. Chem.* **2015**, *27*, 1001–1004. [CrossRef]
21. Harabor, A.; Rotaru, P.; Scorei, R.I.; Harabor, N.A. Non-conventional hexagonal structure for boric acid. *J. Therm. Anal. Calorim.* **2014**, *118*, 1375–1384. [CrossRef]
22. Rotaru, A. Thermal and kinetic study of hexagonal boric acid versus triclinic boric acid in air flow. *J. Therm. Anal. Calorim.* **2017**, *127*, 755–763. [CrossRef]
23. Aghili, S.; Panjepour, M.; Meratian, M. Kinetic analysis of formation of boron trioxide from thermal decomposition of boric acid under non-isothermal conditions. *J. Therm. Anal. Calorim.* **2018**, *131*, 2443–2455. [CrossRef]
24. U.S. Geological Survey. *Mineral Commodity Summaries 2018*; U.S. Department of the Interior: Washington, DC, USA, 2018.
25. Indian Bureau of Mines. *Part-III: Minerals Reviews—Boron Minerals*; Government of India—Ministry of Mines: New Delhi, India, 2017.
26. Scorei, R.I.; Rotaru, P. Calcium fructoborate–potential anti-inflammatory agent. *Biol. Trace Elem. Res.* **2011**, *143*, 1223–1238. [CrossRef]
27. Iavazzo, C.; Gkegkes, I.D.; Zarkada, I.M.; Falagas, M.E. Boric acid for recurrent vulvovaginal candidiasis: The clinical evidence. *J. Womens Health* **2011**, *20*, 1245–1255. [CrossRef]
28. Perelygin, Y.P.; Chistyakov, D.Y. Boric acid. *Russ. J. Appl. Chem.* **2006**, *79*, 2041–2042. [CrossRef]
29. CIA. *The Use of Boron Substances in Fuels*; General CIA Records: Washington, DC, USA, 1955.
30. Lager, D. Evaluation of Thermophysical Properties for Thermal Energy Storage Materials—Determining Factors, Prospects and Limitations. PhD Thesis, TU Wien, Wien, Austria, 2017.
31. Vyazovkin, S.; Chrissafis, K.; Di Lorenzo, M.L.; Koga, N.; Pijolat, M.; Roduit, B.; Sbirrazzuoli, N.; Sunol, J.J. ICTAC Kinetics Committee recommendations for collecting experimental thermal analysis data for kinetic computations. *Thermochim. Acta* **2014**, *590*, 1–23. [CrossRef]
32. Mukhanov, V.A.; Kurakevich, O.O.; Solozhenko, V.L. On the hardness of boron (III) oxide. *J. Superhard Mater.* **2008**, *30*, 71–72.
33. Dressler, W. *Ueber die Flüchtigkeit der Borsäure. neue Bestimmungen des Verteilungsgleichgewichtes zwischen Wasser und Dampf*; ETH Zürich: Zurich, Switzerland, 1945.
34. Pawlek, B. Optimierung des B_2O_3—H_3BO_3 Reaktionssystems zum Zwecke der thermischen Energiespeicherung. Bachelor's Thesis, TU Wien, Wien, Austria, 2019.

35. Reis, J.M.S.M.d. Hydration of Boron Oxide for Thermochemical Energy Storage. Master's Thesis, TU Wien, Wien, Austria, 2018; p. 85.
36. Werner, A.; Karel, T.; Jordan, C.; Deutsch, M.; Winter, F. Verfahren zur thermochemischen Energiespeicherung. Austrian Patent AT 518448 B1, 15 December 2017. Available online: www.patentamt.at (accessed on 21 March 2019).